

Article

Not peer-reviewed version

The Matrix Receptor CD44 Is Present in Astrocytes Throughout the Human CNS and Accumulates in Hypoxia and Seizures

[Osama Al Dalahmah](#) , [Alexander A Sosunov](#) , [Yu Sun](#) , [Yang Liu](#) , Nsikan Akpan , Nacoya Madden , E. Sander Connolly , [Carol M Troy](#) , Guy M McKhann II , [James E. Goldman](#) *

Posted Date: 27 March 2023

doi: 10.20944/preprints202303.0444.v1

Keywords: CD44; astrocytes; hypoxia; seizures; interlaminar astrocytes



Preprints.org is a free multidiscipline platform providing preprint service that is dedicated to making early versions of research outputs permanently available and citable. Preprints posted at Preprints.org appear in Web of Science, Crossref, Google Scholar, Scilit, Europe PMC.

Copyright: This is an open access article distributed under the Creative Commons Attribution License which permits unrestricted use, distribution, and reproduction in any medium, provided the original work is properly cited.

Article

The Matrix Receptor CD44 Is Present in Astrocytes Throughout the Human CNS and Accumulates in Hypoxia and Seizures

Osama Al Dalahmah ¹, Alexander A. Sosunov ², Yu Sun ¹, Yang Liu ³, Nacoya Madden ¹,
Nsikan Akpan ¹, E. Sander Connolly ², Carol M. Troy ^{1,4,5}, Guy M. McKhann II ²
and James E. Goldman ^{1,5,*}

¹ Department of Pathology and Cell Biology, Vagelos College of Physicians and Surgeons, Columbia University Irving Medical Center and the New York Presbyterian Hospital, NY, NY, 10032 USA

² Department of Neurosurgery, Vagelos College of Physicians and Surgeons, Columbia University Irving Medical Center and the New York Presbyterian Hospital, NY, NY, 10032 USA

³ Department of Pathology, Albany Medical Center, Albany, NY 12208, USA

⁴ Department of Neurology, Vagelos College of Physicians and Surgeons, Columbia University Irving Medical Center and the New York Presbyterian Hospital, NY, NY, 10032 USA

⁵ The Taub Institute, Columbia University Irving Medical Center, NY, NY, 10032 USA

* Correspondence: jeg5@cumc.columbia.edu

Abstract: In the mammalian isocortex CD44, a cell surface receptor for extracellular matrix molecules, is present in pial-based and fibrous astrocytes of white matter, but not the protoplasmic astrocytes. In the hominid isocortex, CD44+ astrocytes comprise the subpial “interlaminar” astrocytes, sending long processes into the cortex. The hippocampus also contains similar astrocytes. We have examined all levels of the human CNS and found CD44+ astrocytes in every region. Astrocytes in white matter and astrocytes that interact with large blood vessels, but not capillaries in gray matter, are CD44+, the latter extending long processes into the parenchyma. Motor neurons in the brainstem and spinal cord, such as oculomotor, facial, hypoglossal, and in the anterior horn of the spinal cord, are surrounded by CD44+ processes, contrasting with neurons in the cortex, basal ganglia and thalamus. We found CD44+ processes that intercalate between ependymal cells to reach the ventricle and that show a location-specific presence. We also found a CD44+ astrocyte in the molecular layer of the cerebellar cortex. Protoplasmic astrocytes, which do not normally contain CD44, acquire it in pathologies like hypoxia and seizures.

Keywords: CD44; astrocytes; hypoxia; seizures; interlaminar astrocytes

1. Introduction

The so-called interlaminar astrocytes of the mammalian isocortex were first described well over one hundred years ago [1] and further characterized in recent years [2], [3], [4], [5]. These astrocytes display marked differences from the better-known, bushy, protoplasmic astrocytes of the cortex. They project long, unbranched cell processes, usually oriented orthogonally to the pial surface, through several cortical layers, forming cascades of parallel processes. A subset of astrocytes in the deep cortical layers near the subcortical white matter also project similar, radially-oriented processes into the lower cortical layers. Immunocytochemical studies reveal that these long-process astrocytes contain CD44 [6] [4], a cell surface receptor for extracellular matrix molecules, including osteopontin, hyaluronan, laminin, and integrins [7]. They are different from the protoplasmic astrocytes, which do not contain detectable levels of CD44 [4,8], not only in morphology, but are also low in glutamine synthetase (GS) and the two glutamate transporters, EAAT1 and EAAT2 [4]. However, CD44 can be increased in astrocytes in response to pathological conditions [4,8]. The astrocytes in white matter are also CD44+ [4,8,9].

We have now examined other parts of the human CNS and found that CD44+ astrocytes are common in every part of the CNS, including cortex, striatum, thalamus, brainstem, cerebellum, and

spinal cord. In all areas we found CD44 associated with long-process astrocytes. CD44+ astrocytes populate white matter, subependymal zones, as well as subpial areas. We found that the proximity of CD44+ processes to neuronal cell bodies varies considerably. In particular, unlike neurons in the isocortex and diencephalon, the motor neurons of the brainstem and spinal cord show a close apposition of CD44+ processes, and even were encircled by these processes. We raise the issue of whether this apposition may suggest a novel, intimate relationship between neurons and CD44+ astrocytes for specific neuronal classes.

In this study we have also examined biopsy and autopsy material from individuals who had experienced hypoxic events and seizures and found that protoplasmic astrocytes accumulate CD44 in these pathological conditions,

2. Materials and Methods

Human Autopsy and Biopsy Material

Eight autopsy brains, fixed in 10% formalin for 10 days after removal, were sectioned coronally and samples from all areas of the CNS, including superior frontal, cingulate, and striate cortices with subcortical white matter, hippocampus with temporal isocortex, basal ganglia, thalamus, midbrain, pons, medulla, cerebellum with cortex and dentate nucleus, and spinal cord were removed and embedded in paraffin blocks, cut at 7mm thickness, and mounted on glass slides. Patients' ages ranged from 27 to 74, 6 were female, 2 were male. None of these brains showed evidence of neuropathology except for mild atherosclerosis and arteriolosclerosis and acute but mild hypoxic/ischemic changes. In addition, we sampled sections of anterior striatum from 3 more autopsies (ages in years and sex 1M, 76F, 94F), sections of hippocampus from 8 more autopsies (ages in years and sex 1M, 2M, 5M, 7M, 73M, 71M, 76M, 66M), and sections of spinal cord from 4 more autopsies (ages in years and sex 27F, 66M, 80M, 80M). We also sampled sets of sections of cerebral hemispheres containing the subependymal zone at the lateral ventricle, from 8 fetal and neonatal brains, ranging in age from 19 to 40 weeks of gestation and 1 day to 7 weeks of postnatal life. All autopsies were performed with the consent of the next of kin, and all protocols were approved by the Institutional Review Board of Columbia University Medical Center.

Epilepsy Surgical Specimens

We examined 9 samples of temporal isocortex of patients with mesial temporal sclerosis (ages ranged from 12 – 55; 6M, 3F). We also examined 5 samples of hippocampi from patients with mesial temporal sclerosis (ages ranged from 9 – 66; 3M, 2F) obtained from surgical resections from patients with medically intractable epilepsy. We did not include specimens from seizure patients with brain tumors, vascular malformations, cortical dysplasias, and inflammatory and infectious disorders, although we found that many of them also show CD44+ astrocytes.

Hypoxia Specimens

Eight neurosurgical specimens that represented hypoxic/ischemic insults were selected. We used both the time between the initial clinical presentation and the biopsy and the neuropathology to classify these as acute, subacute, or chronic hypoxic/ischemic changes, acute within a few days and showing eosinophilic neuronal change but no reactivities of blood vessels, astrocytes or microglia, subacute between 10 and 14 days and showing proliferative vasculature and reactive astrocytes and microglia with macrophages, and chronic more than 14 days and showing tissue necrosis with foamy macrophages. Some of the biopsies showed acute and subacute or subacute and chronic changes, indicating progressive changes in the evolution of the lesions. The age range was 19 – 82, 3M, 5F. CD44 positive astrocytes were counted in three 20x power fields from each case. Sample T-tests were performed between pairs of the three groups.

Rodent Hypoxia/Ischemia and Seizure Models

Adult male rats were housed in standard cages with free access to food and water on a 12-h light/dark cycle. All procedures performed on animals were approved by Columbia University's Institutional Animal Care and Use Committee and conducted according to Institutional and Federal guidelines.

Stroke/Transient Middle Cerebral Artery Occlusion (tMCAO)

Rats were subjected to unilateral tMCAO [10]. Wistar rats (275–300 g) were subjected to transient middle cerebral artery occlusion using intraluminal vascular occlusion. Animals were anesthetized with halothane in a mix of 70% nitrous oxide/30% oxygen, core temperatures were maintained at 37 °C throughout the entire procedure and for 60 min after reperfusion. The right common carotid artery, the right external carotid artery, and the right internal carotid artery were exposed and isolated. MCAO was accomplished by advancing a 25 mm 4–0 nylon suture with a blunted silicone tip (outer diameter, 0.38 mm) through an incision in the external carotid artery until the suture was 18 mm past the carotid bifurcation. MCAO was confirmed by transcranial measurements of cerebral blood flow via laser Doppler flowmetry (Periflux System 5000; Perimed, Inc., Järfälla, Sweden). After 120 min, the suture was removed, and reperfusion was confirmed by laser Doppler flowmetry. After 96 h, animals were deeply anesthetized with an overdose of ketamine/xylazine, and perfused with 4% PFA. After perfusion brains were removed and additionally fixed in 4% PFA in PBS for 14–18 h (4°C). 40 µm sections were prepared with a vibratome (Leica VT1000S) and stored in cryoprotectant solution at –20°C. After perfusion brains were dissected and incubated at 4°C with 4% PFA (24 hr), 1x PBS (24 hr), and 30% sucrose in 1xPBS, then embedded in O.C.T. and 20µm cryosections were prepared.

Pilocarpine Induced Status Epilepticus

Seizures were produced in rats with pilocarpine, as described elsewhere [11]. After premedication with scopolamine (5 mg/kg, i.p.) to prevent the effects of peripheral cholinergic stimulation, pilocarpine (330 mg/kg, i.p.) was administered to Sprague-Dawley rats (100–150 g) to induce seizures. Seizures were graded on the modified Racine scale [12] and only animals with grade 4–5 seizures for 2 h were used in experiments. After 2 h of continuous seizures, ketamine (80 mg/kg, i.p.) was administered to stop seizures, and a second dose (40 mg/kg, i.p.) was administered if seizures did not stop in 10 min after the first. After perfusion brains were removed and processed as above.

Immunostaining and Antibodies

Formalin-fixed paraffin-embedded sections were stained using hematoxylin and eosin (H&E). Immunohistochemistry with positive and negative controls was performed using an antibody to CD44 (Roche, mouse monoclonal antibody pre-diluted at 1:100 and run on the Ventana platform using the Ultraview DAB kit). For immunofluorescence staining of the rat MCAO occlusions and pilocarpine-induced seizures, we used a CD44 mouse monoclonal (1:80; clone F10-44-2, Dako) and a glial fibrillary acidic protein (GFAP) rabbit polyclonal (1:1000, Z 0334, Dako, Carpinteria, CA). Secondary antibodies conjugated to fluorophores: anti-mouse Alexa Fluor 488, 594, and 633, anti-rabbit Alexa Fluor 488, 594, and anti-goat Alexa Fluor 488, 594, 633; all from goat or donkey (1:300, ThermoFisher Scientific, Eugene, OR). After blocking with 10% normal goat (or donkey) serum (30 min, RT), free-floating sections were incubated in a mixture of primary antibodies overnight (4°C). Alexa Fluor-conjugated secondary antibodies were used for 1h at RT. For visualization of nuclei DAPI (5 µg/ml; D9542, Sigma-Aldrich) was applied with secondary antibodies. Blocking serum, primary, and secondary antibodies were applied in 0.2% Triton X-100 in PBS. Sections for fluorescence microscopy were mounted on slides in Vectashield (Vector Laboratories, Burlingame, CA). To control for the specificity of immunostaining, primary antibodies were omitted and substituted with appropriate normal serum. Slides were viewed using a confocal microscope (Nikon Ti Eclipse). For immunofluorescence staining of cerebellar sections we used 5–7µm thick FFPE sections, which were

immunostained on a Leica Bond RXm™ which the following modifications: after blocking in 10% donkey serum, sections were incubated with rabbit anti CD44 monoclonal antibody (abcam cat#ab101531, 1:100) and chicken anti-GFAP (Abcam cat# ab4674, 1:1000) using antigen retrieval with Leica ER2 antigen retrieval buffer for 20 minutes. The secondary antibodies were 488 donkey anti chicken and 568 donkey anti rabbit (1:500). Images were acquired at 40X on a Leica DMi8 Thunder system.

Quantification of CD44 in Hypoxia Sections

All CD44+ astrocytes were counted in 20X objective fields on a Nikon BX43 microscope. Three fields were counted per slide. Statistical analysis was done using ANOVA. Data is shown as mean \pm SEM.

3. Results

CD44+ Astrocytes in the Normal Human CNS

Specificity of CD44 Immunostaining for Astrocytes

CD44 co-localized with GFAP in the isocortex and hippocampus [4]. Neurons, oligodendrocytes, myelin, and microglia were CD44-negative, although macrophages and classes of lymphocytes were positive. None of the autopsy brains we examined for the characterization of CD44+ astrocytes in non-pathological tissues had any neuropathological findings, including areas of macrophage accumulation, lymphocyte infiltration, or astrocyte scars.

Isocortex

The cellular architecture of CD44+ astrocytes has been described in the isocortex [4,6,13] and matches that of the well-known interlaminar astrocytes with cell bodies at or near the pial surface and also astrocytes around large blood vessels. Note that the CD44+ astrocyte cell bodies sit at or near the pial surface (Figure 1). Isocortical neurons are not apposed or surrounded by CD44+ processes, including the Betz cells of the primary motor cortex (see below, in contrast with brainstem and spinal cord motor neurons, which are surrounded by CD44+ processes).

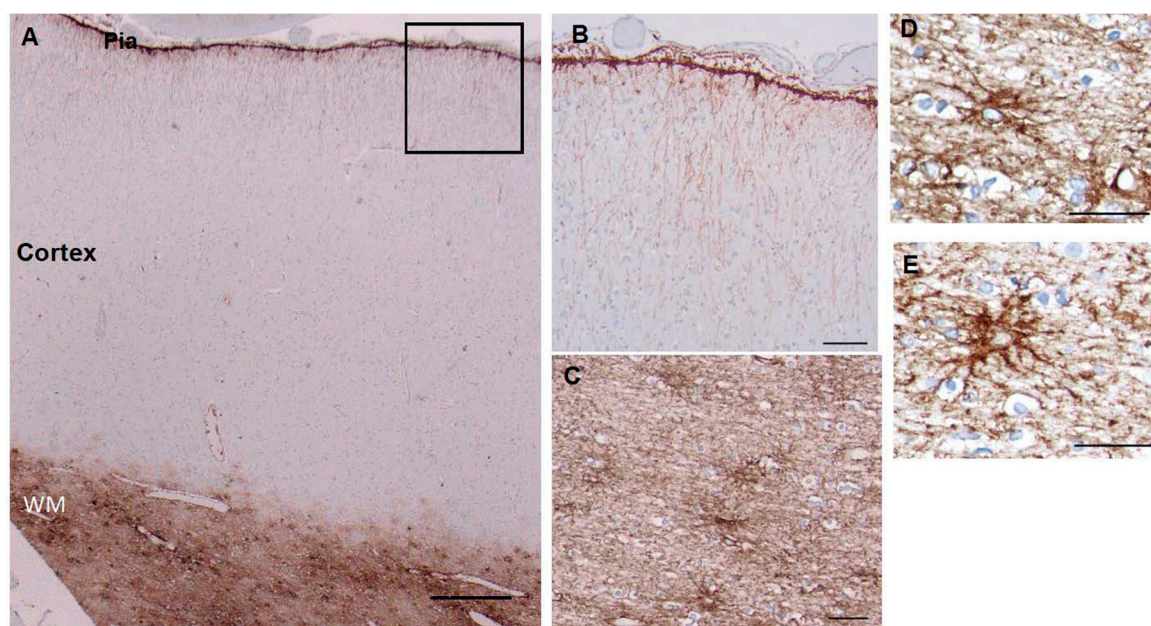


Figure 1. Superior frontal cortex shows CD44 positivity in subpial (Pia), interlaminar astrocytes and white matter astrocytes (WM), but not in the protoplasmic astrocytes of the cortex (A). Higher magnification of boxed area in A to show the long interlaminar processes, radial to the pial surface

(B). Subcortical white matter, showing dense astrocyte processes, many of which course along axonal tracts (C). Higher magnification of white matter astrocytes, which extend long processes in many directions, although the longest processes are roughly parallel and in the direction of axonal tracts (D, E). Scale bars: A 250 μ m, B 50 μ m, C 25 μ m, D, E 20 μ m.

Subcortical White Matter

The fibrous astrocytes of white matter were CD44+ in every area of the CNS. These astrocytes were complex in shape, extending long processes along axonal tracts and also shorter processes in other orientations as well (Figure 1). As we have noted previously [4], some of the subcortical white matter astrocytes projected long, unbranched, radially-oriented processes into the lower cortical levels (Figure 1). A number of other CNS areas also showed projection of long CD44+ processes from white matter into gray matter (for eg. see dentate nucleus, below).

Striatum

CD44+ astrocytes occupied the subependymal layer forming a dense matrix (Figure 2). From there, long-processes of CD44+ astrocytes projected into the caudate. In examining the ependymal lining we found that CD44+ processes intercalated between the CD44-negative ependymal cells (Figure 2). In the ependymal lining over the caudate nucleus these processes are more frequent dorsally than ventrally. We observed this dorsal-ventral gradient in 11/11 sections of anterior caudate, in patients ranging in age from 1 year to 94 years. In addition, we examined the germinal matrix at the angle of the lateral ventricle in 8 fetal brains, aged 19 to 40 weeks of gestation and 4 postnatal brains, aged 1 day to 7 weeks. All showed CD44+ processes in between ependymal cells (Supplemental Figure S1). In some cases it was possible to trace these processes into the underlying subependymal zone. CD44+ astrocytes also appeared in the striatal white matter, their processes parallel to the pencil fiber axons striatum and in the internal capsule, as expected. Protoplasmic astrocytes of the gray matter were CD44-negative. No caudate or putamen neurons were surrounded by CD44+ processes.

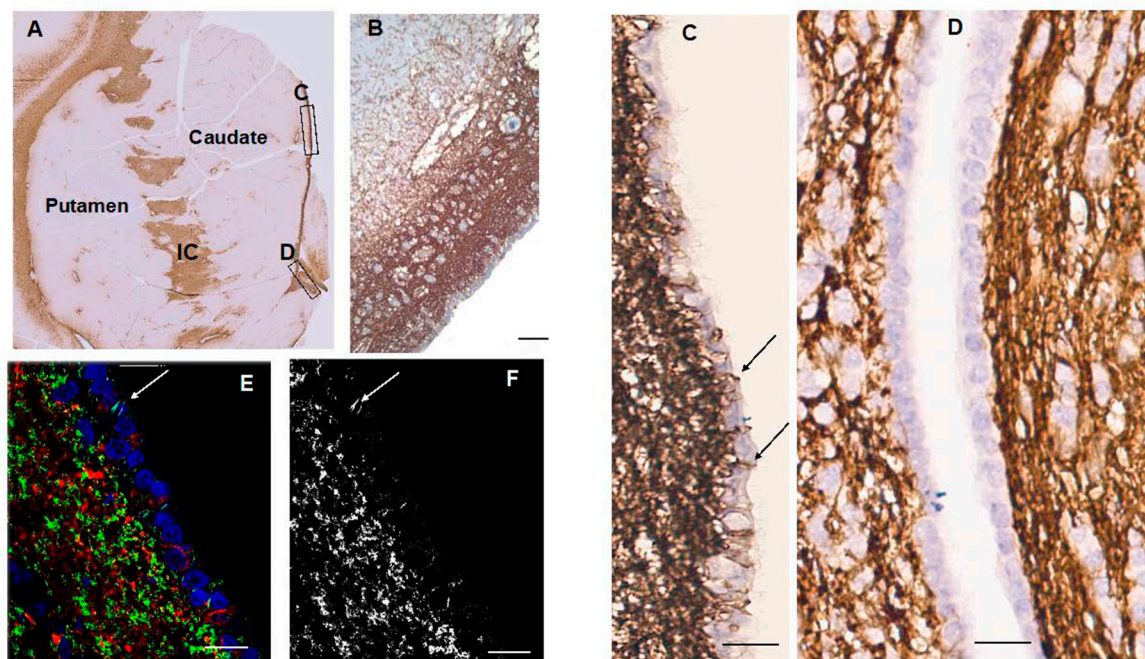


Figure 2. Caudate and putamen show CD44 positivity in the subependymal region, the internal capsule (IC) and the white matter fibers of the striatum (A). Higher magnification of the subependymal regions shows a dense network of CD44+ processes, some of which extend into the caudate (B). Higher magnification of the subependymal network (C, D). CD44+ processes extend between ependymal

cells over the dorsal caudate to the ventricle in the dorsal (C), but far fewer of these are present in more caudal areas (D). Confocal imaging also reveals CD44⁺ processes in between ependymal cells (arrows) (E, CD44 (green), GFAP (red), DAPI (blue), (F, CD44⁺ only). Scale bars: A 250 mm, B 100 mm, C,D,E,F 20 mm.

Thalamus

In paraventricular thalamic nuclei, there was a dense network of CD44⁺ processes in the subependymal zone (Figure 3). CD44⁺ processes also intercalated between ependymal cells, (Figure 3). Astrocytes surrounding large thalamic vessels appeared CD44⁺ and sent long processes into the thalamic neuropil (Figure 3). There were more CD44⁺ astrocytes dispersed throughout thalamic nuclei than in the striatum. This may correlate with the large numbers of groups of myelinated axons that course through the thalamus, although some CD4⁺ astrocytes appear to be unassociated with white matter or blood vessels (Figure 3). The anterior nucleus was relatively poor in these astrocytes, whereas the lateral nuclei and the subthalamic nucleus contained more of them. Thalamic neurons were not surrounded by CD44⁺ processes, however. In the lateral geniculate nucleus (LGN), the white matter between layers contained CD44⁺ astrocytes, which extended long processes into the neuronal layers (Figure 3). The large neurons of the magnocellular layers I and II were surrounded by CD44⁺ staining, while the small neurons in the other layers were not (Figure 3).

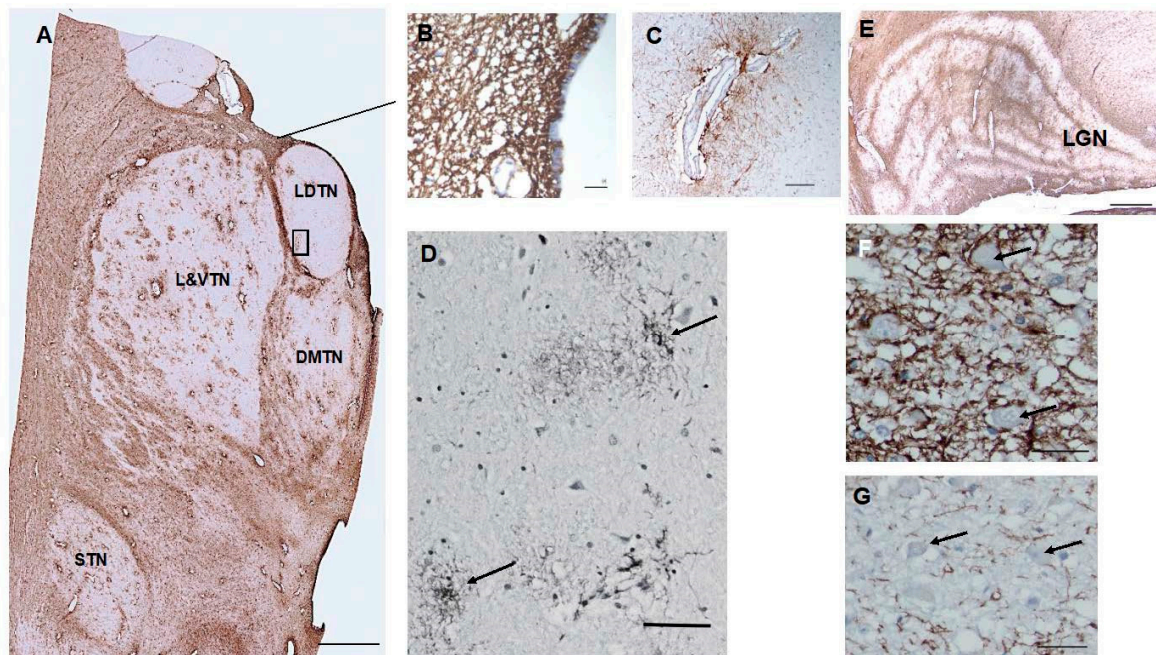


Figure 3. The anterior thalamus, including the latero-dorsal (LDTN), dorso-medial (DMTN), and latero-ventral (L&VTN) nuclei and the subthalamic nucleus (STN) show CD44 positivity around blood vessels and in white matter striae (A). CD44⁺ processes intercalate between ependymal cells, (B). Higher magnification of the boxed area in (A) to show a large vessel surrounded by CD44⁺ astrocytes, which send long unbranched processes into the parenchyma (C). Some of the CD44⁺ astrocytes in the L and VTN do not apparently contact blood vessels (D). Myelinated fiber bands of the LGN are CD44⁺ (E). CD44⁺ surrounds magnocellular neurons ((F), but not parvocellular neurons (G). Scale bars: A 5mm, B 10 mm, C, D 50 mm, F,G 20 mm.

Hypothalamus, IIIrd Ventricle

As in other paraventricular areas, there was a dense subependymal network of CD44⁺ processes and extension of long, unbranched processes from this into the parenchyma (Supplemental Figure S2). The larger vessels were surrounded by CD44⁺ astrocytes, which sent long processes into the neuropil. The ependymal lining of the third ventricle contained CD44⁺ processes intercalating

between ependymal cells, although the numbers appeared sparser than those over the rostral caudate. Neurons of the para- ventricular nuclei of the hypothalamus were completely or partially surrounded by CD44+ processes (Supplemental Figure S2).

Hippocampus

As described [4], CD44+ astrocytes in the stratum oriens projected long processes through the depth of the pyramidal layer of CA1–CA3 and subiculum, ending at the border of the stratum radiatum (Figure 4). CD44+ astrocytes were localized to the molecular layer of the dentate gyrus, in which processes of astrocytes in the subgranular layer extended through the molecular layer (Figure 4). CD44+ astrocytes with long processes were also present in the stratum radiatum and in the hilus of the dentate (Figure 4). CD44+ astrocytes occupied the stratum lacunosum, the white matter tract from the entorhinal cortex. Pyramidal neurons were not surrounded by CD44+ processes (Figure 4).

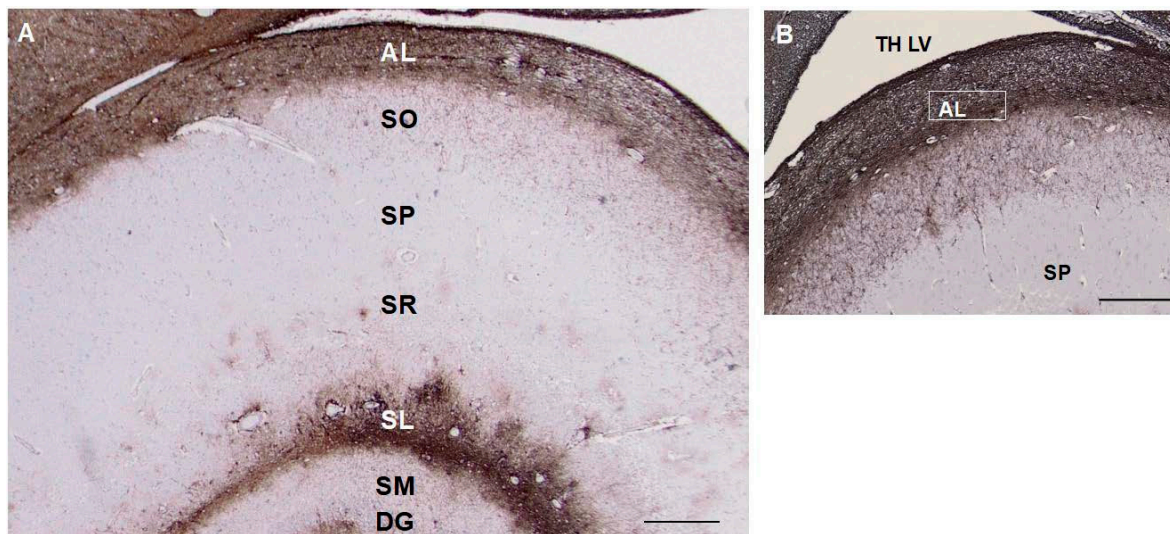


Figure 4. A section through the layers of the hippocampus show CD44 positivity in the alveus (AL) and stratum lacunosum (SL). Thin, unbranched CD44+ processes run through the stratum oriens (SO) toward the pyramidal layer. CD44+ processes do not surround pyramidal cells. Astrocytes in the stratum pyramidale, stratum radiatum (SR), and stratum moleculare (SM) show little CD44 reactivity. CD44+ astrocyte processes course through the dentate gyrus (DG) (A, B). Scale bars: A 250 mm, B 200 mm.

Cerebellum

A. Cortex – We found cell bodies of CD44+ cells located either at the pial surface or just below it (Figure 5). Their processes ran parallel to the pia, although some extended radially toward the Purkinje cell layer. The granule cell layer itself contained a network of CD44+ processes from the velate astrocytes, the astrocytes that populate this layer, surrounding groups of granule cells, but not individual granule cells (Figure 5 and Supplemental Figure 3). The spatial relationship of Purkinje cells to CD44+ processes seemed to vary. Some were not surrounded by CD44+ processes, although a few processes closely traveled by the lateral aspects of Purkinje cells, while others appeared to be surrounded (Supplemental Figure S3). CD44+ processes extended radially from the granule cell layer into the molecular layer (Supplemental Figure 3) indicating that some of the thin processes in the molecular layer had their origins in the granule cell layer. Moreover, in the Purkinje cell layer, a small subset of Bergmann glia, which send long GFAP+ process all the way to the pial surface, were CD44+ (Supplemental Figure S4). As anticipated, white matter of the cerebellar cortex contained CD44+ astrocytes.

B. Dentate nucleus – The white matter surrounding the dentate nucleus, like other white matter in the CNS, was CD44+. Thin CD44+ processes entered and sometimes crossed the dentate nucleus and occasionally enwrapped some dentate neurons, but not others (Figure 5).

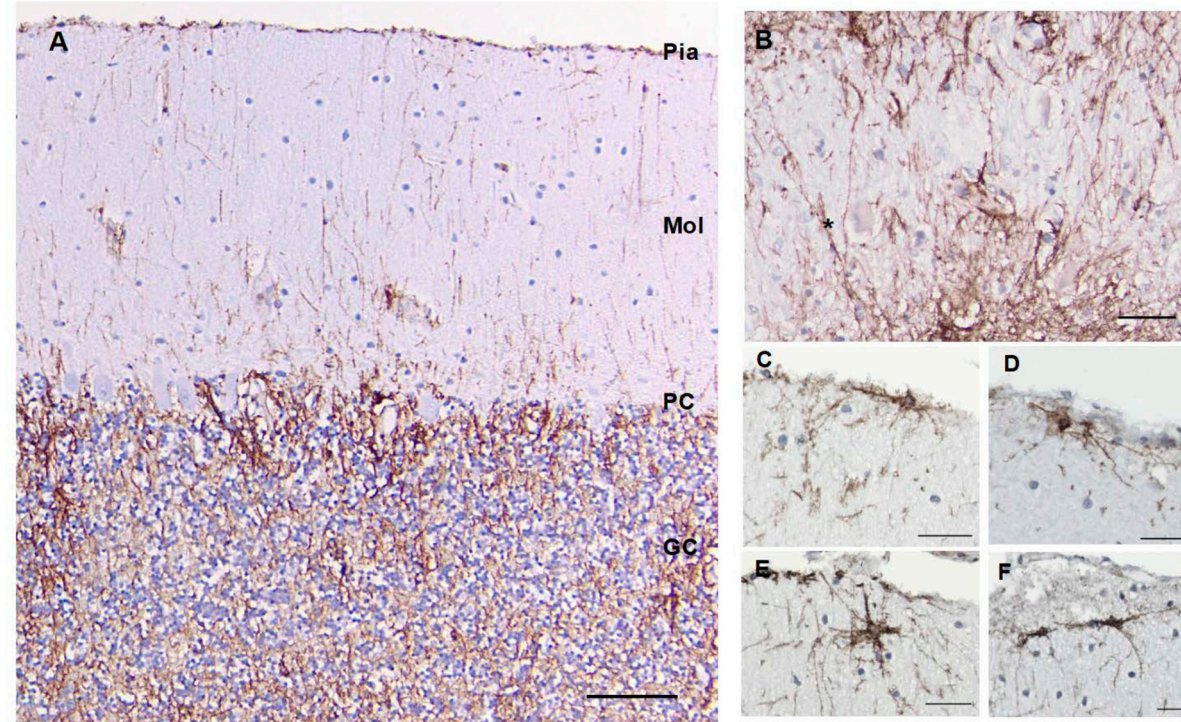


Figure 5. A section through the cerebellar cortex shows CD44+ long processes arising from the pial surface and entering the molecular layer (A). Some appear to begin in the granule cell layer and project into the molecular layer (see Supplemental Figure 3E). Fine CD44+ processes course through the granule cell layer, surrounding groups of granule cells, but do not surround individual granule cells. CD44+ processes run through the dentate nucleus, but do not surround dentate neurons (*) (B). CD44+ astrocytes at or near the pial surface of the molecular layer extend processes parallel to the pia or into the molecular layer (C-F). Molecular layer (Mol), Purkinje cell layer (PC), granule cell layer (GC). Scale bars: A 100 μ m, B, C-F 20 μ m.

Brainstem

Many areas of the brainstem contained CD44+ astrocytes cell bodies and processes, in part due to the abundance of white matter pathways. In the midbrain, white matter pathways such as the cerebral peduncles, the lateral and medial lemnisci, and the superior cerebellar peduncle decussation were all CD44+ (Figure 6). The red nucleus contained many CD44+ astrocytes, likely correlating with the myriad of myelinated axon bundles, but neurons were not surrounded by CD44+ processes. The cell bodies of motor neurons of the oculomotor nucleus were in close contact with CD44+ processes, in some cases enwrapped by them (Figure 6). The substantia nigra contained many CD44+ astrocytes, but nigral neurons were not enwrapped by CD44+ processes (Figure 6).

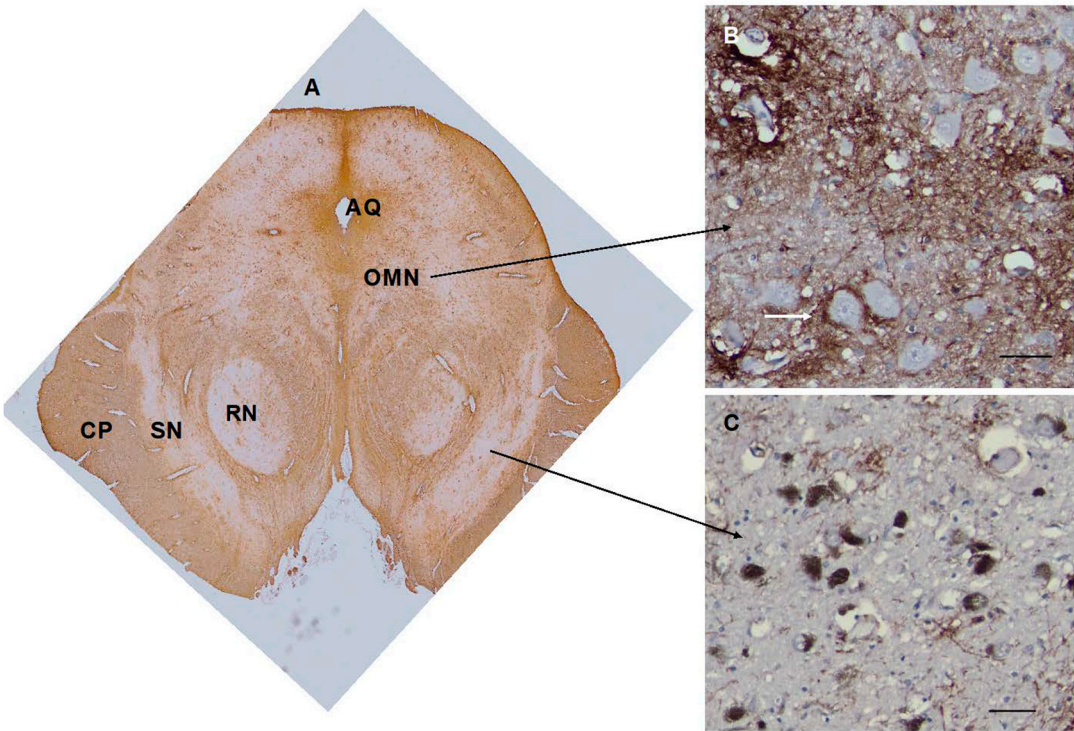


Figure 6. The midbrain appears complex, with CD44 staining of white matter tracts such as the cerebral peduncles (CP). The red nucleus (RN) contains CD44+ astrocytes. The substantia nigra appears relatively free of CD44+ staining (A). Neurons of the oculomotor nucleus (ON) are surrounded by CD44+ staining (B). Neurons of the substantia nigra are not (C). Scale bars: B,C 25 mm.

The medulla also contained CD44+ astrocytes in white matter tracts (Figure 7). Neurons of the hypoglossal nucleus, the dorsal motor nucleus of the vagus, the nucleus ambiguus, but not the solitary tract nucleus or trigeminal nuclei, were surrounded by CD44+ processes (see Table 1 for a list of neurons that are and are not surrounded).

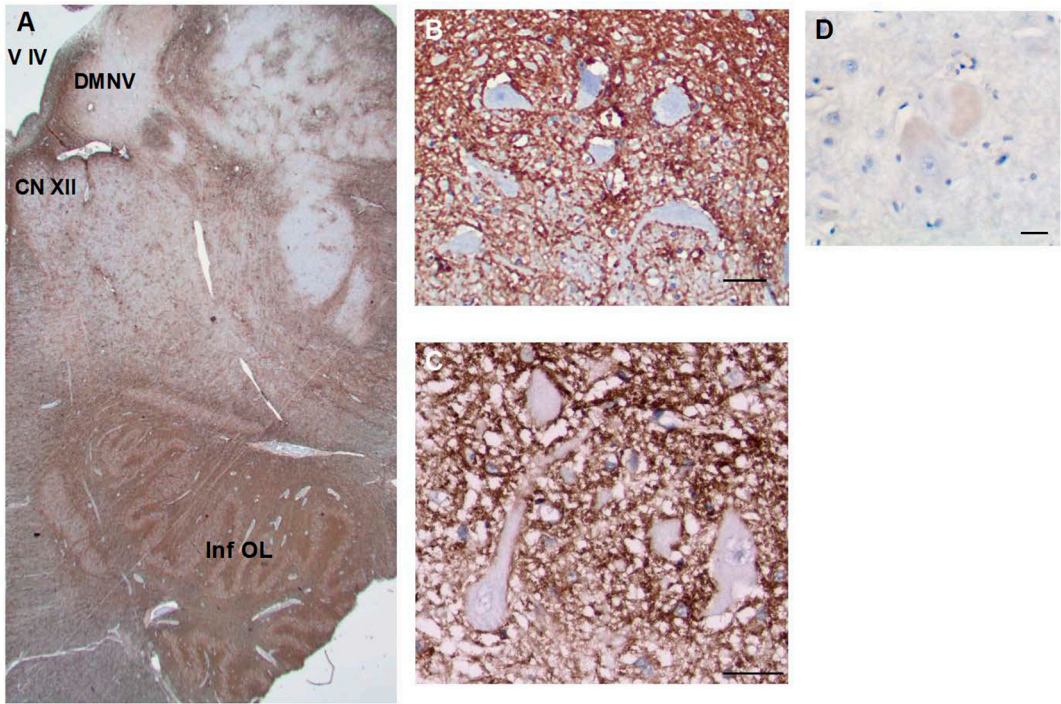


Figure 7. The medulla contains many CD44+ processes, including white matter tracts. Motor neurons of the hypoglossal nucleus (B) and dorsal motor nucleus of the vagus (C) are surrounded by CD44+ processes. In contrast, Betz cells of the motor cortex are not surrounded by C44+ processes (D). Fourth ventricle (V IV), Hypoglossal nucleus (CNXII), dorsal motor nucleus of the vagus (DMNV), inferior olivary nucleus (Inf OL). Scale bars: B, C 10 mm, D 50 mm.

Spinal Cord

The CD44 immunostaining of the spinal cord revealed CD44+ astrocytes in gray and white matter (Figure 8). Motor neurons of the anterior horn were in close contact with CD44+ processes, in some cases enwrapped by them (Figure 8). We found these contacts in all cord levels, cervical, thoracic, and lumbar, the latter containing the nucleus of Onufrowicz. Neurons of the nucleus intermediolateralis and Clarke's column were also surrounded by CD44+ processes. The substantia gelatinosa did not contain CD44+ astrocytes.

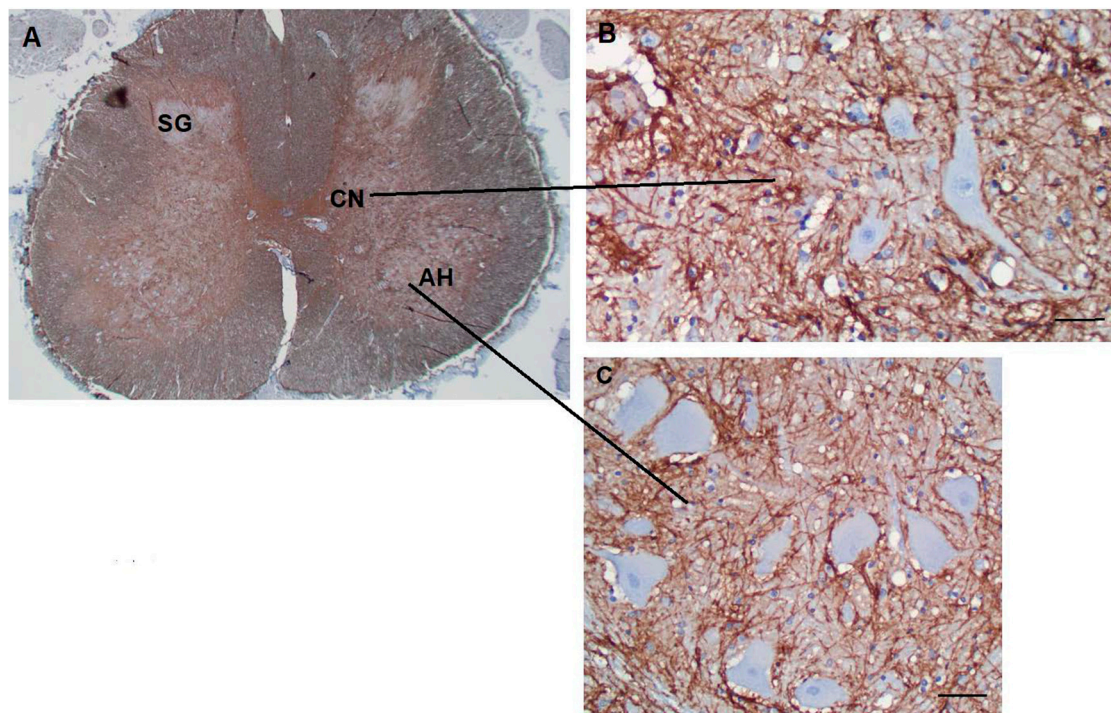


Figure 8. A section through the thoracic spinal cord shows many CD44+ processes, including white matter tracts (A). The substantia gelatinosa contains fewer CD44+ astrocytes. Motor neurons of the anterior horn (B) and neurons of Clarke's nucleus (C) are surrounded by CD44+ processes. Substantia gelatinosa (SG), Clarke's nucleus (CN), Anterior horn (AH). Scale bars: B,C 20 mm.

CD44+ Astrocytes in the Hypoxic Cortex

Protoplasmic astrocytes of the isocortex are not normally CD44+, but acquire CD44 in hypoxic/ischemic lesions. We examined by immunohistochemistry a series of neuro-surgical and autopsy isocortical specimens from patients with well-defined clinical histories for the onset of hypoxic/ischemic events, allowing us to gauge the timing of CD44 accumulation. Very few CD44-positive astrocytes were present in acute infarcts (1-2 days). However, within several days after the insult, some cortical astrocytes began to show weak staining for CD44, and by 12-14 days, many astrocytes in the affected cortex stained strongly (Figure 9, Supplemental Figure S5). The CD44+ astrocytes resided in the penumbra of infarcts or within hypoxic lesions that did not contain necrosis.

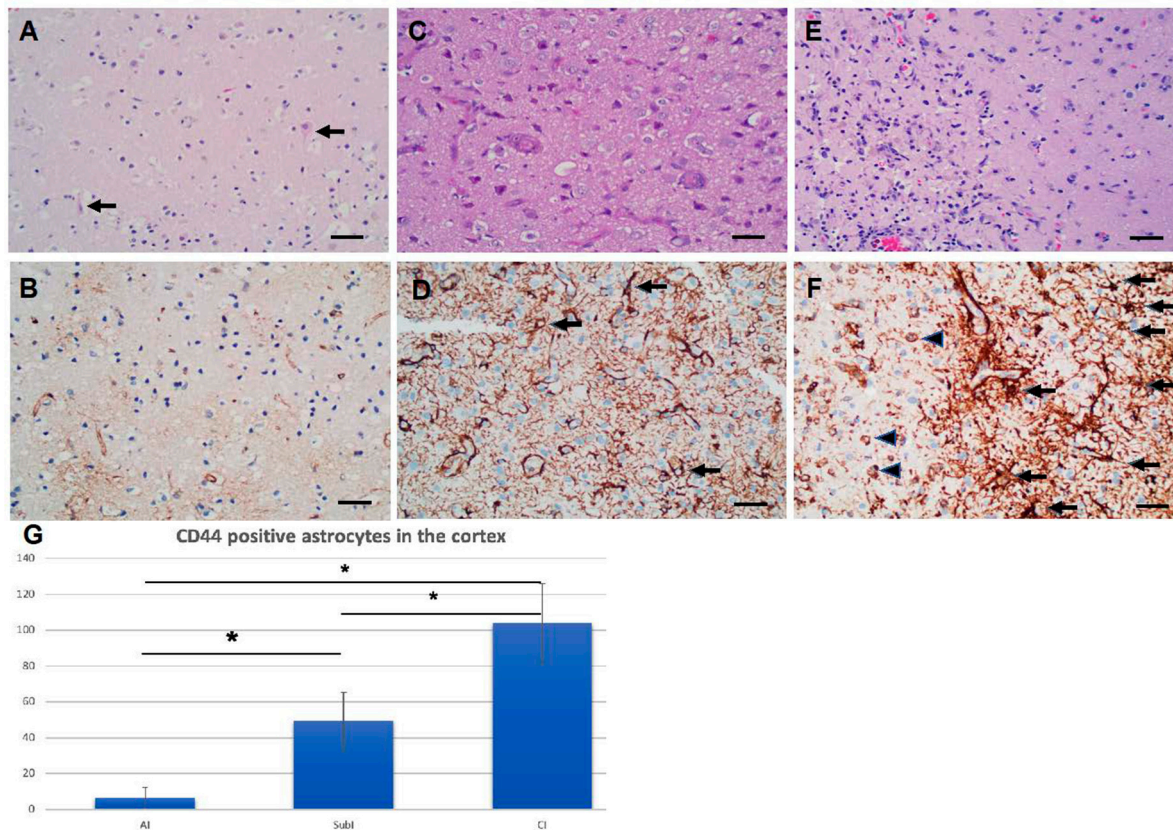


Figure 9. Astrocytes increase CD44 levels in hypoxic ischemic conditions. A and B, C and D, E and F acute, subacute and chronic infarcts, respectively (H&E). Eosinophilic neurons (arrows) are seen in A. Proliferative vasculature is present in. Foamy macrophages are more pronounced in E in an area of necrosis (left side of the panel). B, D, and F are the corresponding immunohistochemical stains for CD44 of A, B and C, respectively. CD44-positive astrocytes are highlighted (black arrowheads). Macrophages (arrowheads) are also positive for CD44. The vessels are outlined by CD44 stain. Scale Bars: 20 mm. (G) The numbers of CD44-positive astrocytes increase as infarcts evolve (average numbers in three 20x fields/specimen). AI: acute infarct; SubI: subacute infarct; CI: chronic infarct. (* $p < 0.01$, SubI vs. AI, * $p < 0.01$, CI vs. AI; * $p < 0.01$, CI vs. SubI). ANOVA, showing means \pm SEM.

We also examined a rat model of brain ischemia, generated by unilateral transient occlusion of middle cerebral artery. After 7 days, many of the cortical astrocytes, which had previously been CD44 negative, became CD44+ (Figure 11). Cortical astrocytes on the contralateral side remained CD44 negative.

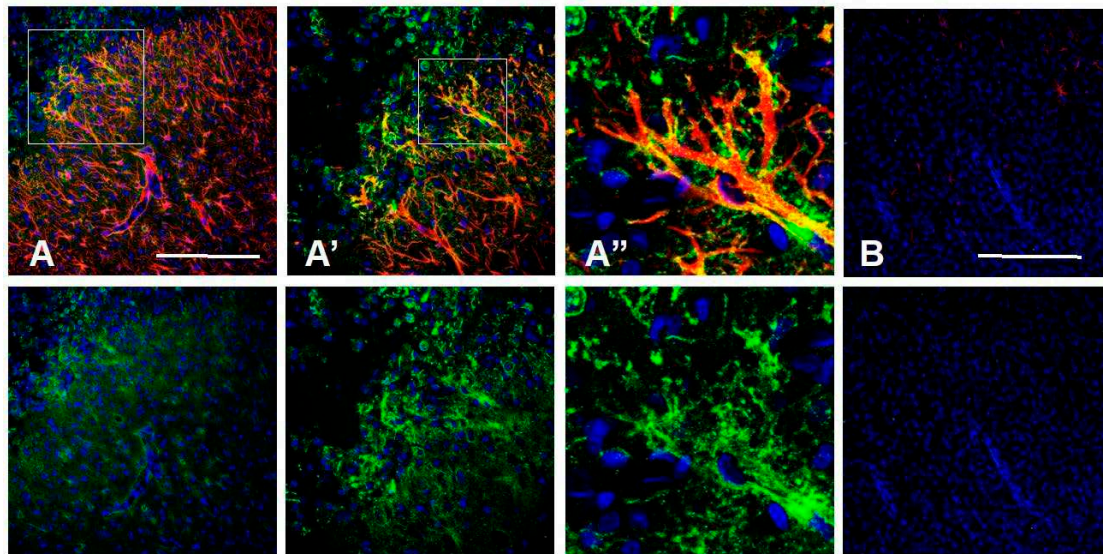


Figure 10. Isocortical astrocytes become CD44+ 7d after transient MCA occlusion. Lower magnification (A) and higher magnifications of boxed area (A', A'') show CD44+/GFAP+ astrocytes in the cortex. The contralateral cortex does not show CD44+ astrocytes (B). Top row shows CD44 (green), GFAP (red), DAPI (blue), bottom row shows only CD44 and DAPI of the same fields. Scale bars: 240 μ m.

CD44+ Astrocytes in Epilepsy

Because of the reports of CD44 increase in epilepsy [14,15] and in tuberous sclerosis, which is often accompanied by seizures [13,16], we examined a group of neurosurgical specimens removed from patients with temporal lobe epilepsy, both the hippocampi and the adjacent temporal isocortex for CD44+ astrocytes. The hippocampi showed an increase in CD44 immunostaining in all sectors (Figure 12, and compare with Figure 4). CD44 staining of all 4 resections that contained hippocampus revealed that neurons of the pyramidal cell layer were surrounded by CD44+ processes, a morphology not present in the normal brain (Figure 12). The temporal isocortex showed a variety of increased CD44 in cortical astrocytes (Figure 13), although more appeared severe than moderate or low. We do not have the full clinical histories of all of these patients, however, and so cannot try to correlate the extent of CD44 staining with clinical behavior. Furthermore, sampling is an issue, since we do not know how far away the cortical samples were taken from the hippocampus. Thus, we can conclude that in some of these individuals there has been a transformation of CD44-negative protoplasmic astrocytes to CD44+ astrocytes. Interestingly, some of the CD44+ cortical astrocytes had extended long processes (Figure 14), an abnormal morphology for protoplasmic astrocytes, which do not extend such processes.

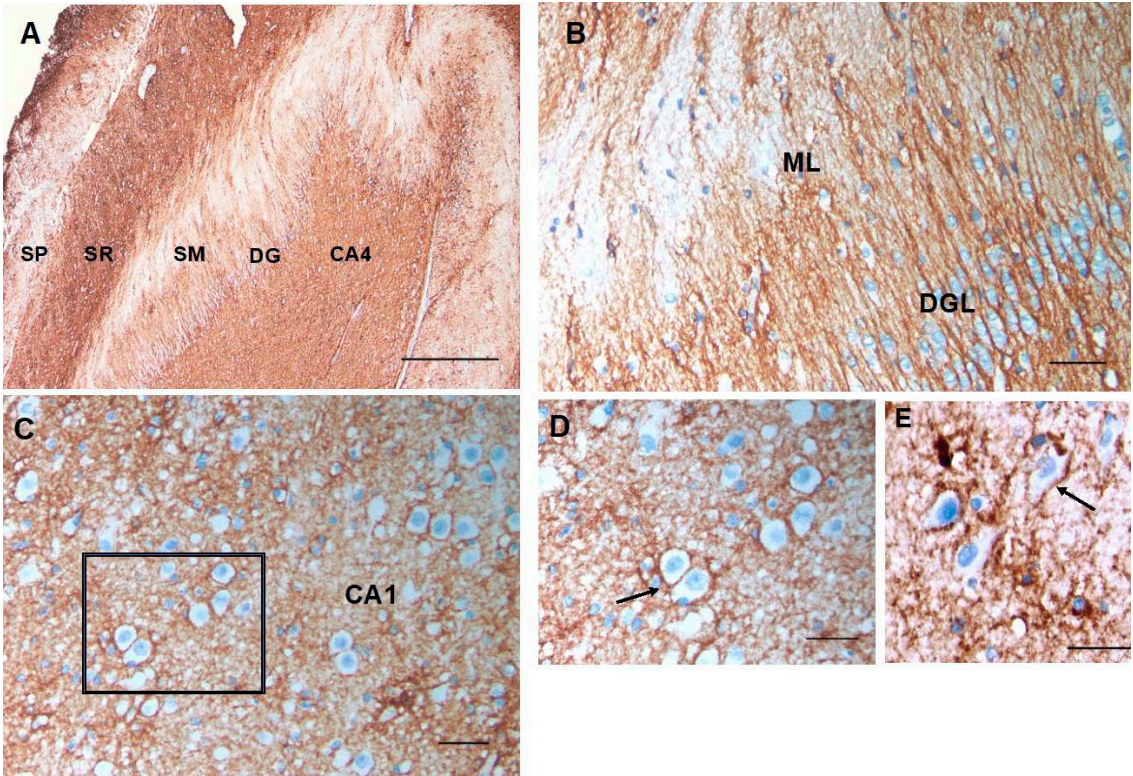


Figure 11. Changes in CD44 in the sclerotic hippocampus in mesial temporal lobe epilepsy. Compare with Figure 4. There is an increase in CD44 in all layers (abbreviations as in Figure 4) (A). The radially oriented astrocyte processes in the dentate granule layer (DGL), which extend into the molecular layer (ML) are CD44+ (B). Pyramidal neurons, which are normally not surrounded by CD44+ processes, have become so (C, D). (D) is the boxed area in (C). Pyramidal neurons are surrounded by CD44+ processes in another specimen (E). Scale bars: A 200 mm, B 25 mm, C 25 mm , D, E 20 mm.

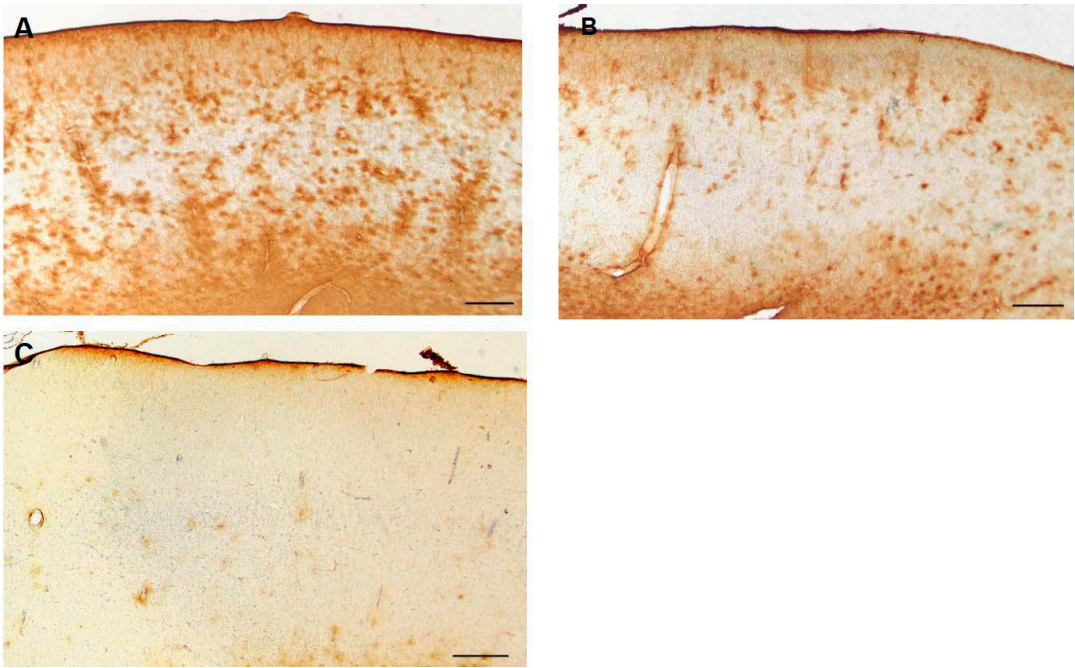


Figure 12. Temporal isocortex in individuals with temporal lobe epilepsy. In some resections, many astrocytes have become CD44+ (A). In others, fewer are CD44+ (B, C). The pial surface of the cortex is at the top. Scale bars: A, B, C 250 mm.

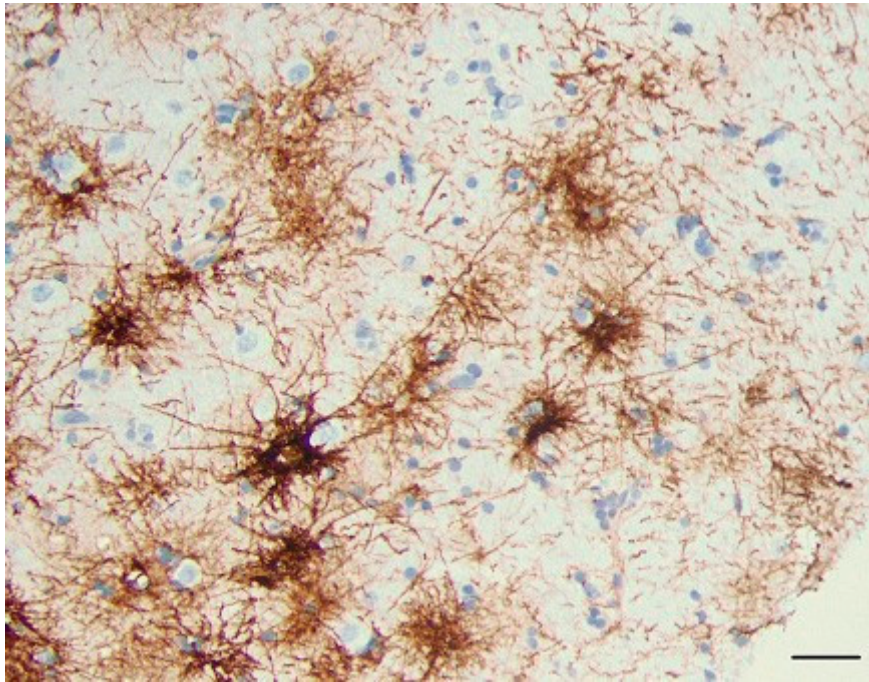


Figure 13. A higher magnification of CD44+ astrocytes in the temporal isocortex reveals that many of them have extended long processes, an abnormal morphology for protoplasmic astrocytes. Scale bar: A 20 mm.

We also examined the isocortex of rats who had been subjected to pilocarpine-induced seizures. The normal rat cortex contains CD44+ astrocytes at the pial surface and in the subcortical white matter, but the protoplasmic astrocytes in the cortex do not contain detectable CD44. However, following pilocarpine-induced seizures, cortical astrocytes began to acquire CD44 from day 4 after pilocarpine and preserved expression in these astrocytes up to a year later (Figure 15).

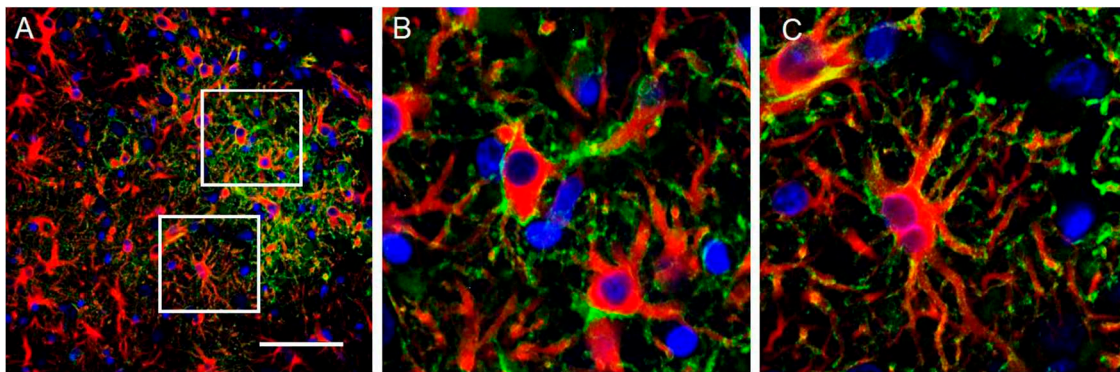


Figure 14. CD44+ astrocytes in the cortex of rats 7 days after pilocarpine-induced seizures. All CD44+ astrocytes are also GFAP+ (A, B, C). (B) and (C) represent boxed areas of (A). GFAP (red), CD44 (green), DAPI (blue). Scale bar: 70 mm.

4. Discussion

CD44+ Astrocytes Populate the Entire Human CNS

In examining astrocytes throughout the human CNS we found not only that they populate every area, but also that they are morphologically remarkably heterogeneous.

Interlaminar Astrocytes

Long-process astrocytes in the isocortex have been known for over a century in human and other large mammalian brains. The smaller brains, such as those of rodents, do not show these, although astrocytes at the pial surface are also CD44+, as are white matter astrocytes (our unpublished observations). That the morphology is species dependent is implied by studies that produce long-process astrocytes in the mouse after transplanting human induced pluripotent stem cells into the mouse cortex [17], suggesting that human long-process astrocytes are intrinsically programmed to assume this morphology.

Our findings in the isocortex and hippocampus confirm and extend those of our previous work [4] and we now show that CD44+ astrocytes are found throughout the human CNS axis. Long, unbranched processes lacking a bushy appearance distinguish these from the protoplasmic astrocytes of gray matter, which are CD44-negative. The presence of CD44, however, does not imply that all of these astrocytes represent a single population. For example, the “fibrous” astrocytes of the white matter may be different from the subpial, long process astrocytes and the astrocytes that occupy subependymal locations or the astrocytes that wrap around brainstem and spinal cord neurons. Single cell and single nucleus RNA sequencing of the human CNS may indeed separate these populations, now defined by location and morphology, into multiple groups with different transcriptional profiles.

The pial based CD44+ interlaminar astrocytes and the white matter based astrocytes with processes entering the lower cortical layers may represent remnants of the outer radial glia and ventricular radial glia that develop late in gestation in the human hemispheres after neuronal migration has taken place [18].

Neurons Surrounded by CD44+ Processes

One of the unexpected findings was that in the brainstem and spinal cord, many neurons are surrounded by CD44+ processes. The presence of CD44+ processes surrounding motor neurons of the brainstem and spinal cord has not been previously reported. We did not see this phenomenon in isocortical, diencephalic, thalamic, or hippocampal neurons. Exceptions to this observation are the neurons of Clarke’s nucleus, large, Nissl-rich neurons that receive input of large synapses from tendon organs and muscle spindles and the magnocellular neurons of the LGN. Also, some Purkinje cells appear to be partially surrounded by CD44+ processes. Whether these contacts between neurons and CD44+ astrocytes are functionally important awaits further investigation. Studies of carcinoma cells may give one clue to this interaction [19]. The intracellular domain of CD44 (CD44ICD) acts as a transcription factor for genes that contain a CD44ICD response element, and promotes the expression of pyruvate dehydrogenase kinase, (*PDK1*), 6-phosphofructo-2-kinase (*PFKFB4*), and aldolase C (*ALDOC*). Miletti-Gonzalez et al. [19] suggest that upregulation of these genes implies that CD44 may play a role in oxidative glycolysis, since *PDK1* promotes the conversion of pyruvate to lactate, a molecule known to be transferred from astrocytes to neurons to promote energy. Since these studies were done in cancer cell lines it would be interesting to test what genes the CD44ICD promotes in CD44+ astrocytes.

We found that hippocampal pyramidal neurons in TLE were also surrounded by CD44+ processes. We interpret this as the acquisition of CD44 by normal protoplasmic astrocytes whose processes normally contact neurons. Thus, pathological situations may promote this enwrapping. Whether this represents new process formation by astrocytes will await further investigation. What functional significance this enwrapping has will be interesting to examine.

Subependymal Astrocytes

Another unexpected finding was the dense matrix of CD44+ processes in the subependymal region. Because of the density it was difficult to follow individual astrocyte morphologies, even with confocal microscopy. We did notice that CD44+ processes appeared to intercalate between ependymal cells, which themselves were CD44-negative. This morphology and location seems reminiscent to that of neural stem cells in the adult mouse brain and subependymal astrocytes in human brain, which can function as neural stem cells [20–22]. However, further comparison between

these human CD44+ subventricular cells and neural stem cells will have to await much further analysis.

Thalamic Astrocytes

Many of the CD44+ astrocytes in the thalamus and subthalamic nucleus are attached to large blood vessels, as seen elsewhere in the CNS. Other CD44+ astrocytes may be associated with myelinated fiber bundles. It appeared, however, that there were other CD44+ astrocytes that were not associated with vessels or bundles. It is possible that these represent another astrocyte “type”, further adding to the heterogeneity of these cells and gives further impetus to investigating the molecular signals that regulate CD44 expression in human astrocytes.

Cerebellar Astrocytes

The cerebellar cortex contains several types of CD44+ astrocytes. Vellate astrocytes, which have unique morphologies, send out many processes to enwrap clusters of granule cells [23]. Astrocytes in the upper part of the molecular layer, near the pial surface, are not well described, to our knowledge. There are thin, radial, CD44+ processes passing through the molecular layer. The source of these is not clear, although some are contiguous with CD44+ processes in the granule cell layer. Such thin processes were described by Cajal, who thought from his Weigert stains that they originated from astrocytes in the granule cell layer or the underlying white matter [24]. These processes are far less dense than those of Bergmann glia, but some may represent a subpopulation of Bergmann astrocytes. *Astrocytes with vascular contacts*

We also observed that CD44+ astrocytes surround large blood vessels, sending long processes radially into the neuropil. In contrast, astrocytes that contact capillaries are CD44-negative. Thus, astrocyte contacts with large vessels may promote the CD44+ phenotype, or contact with capillaries may repress the phenotype and promote the characteristics of protoplasmic astrocytes. If CD44 is involved in the interaction, it may bind to the matrix surrounding large vessels that is not located near capillaries.

Hypoxia

We found that hypoxic/ischemic insults caused the protoplasmic astrocytes of the isocortex to become CD44+. Studies of tumor cell lines suggest mechanisms underlying this change. Thus, hypoxia regulates CD44 expression via HIF-1α in breast cancer [25] and gastric cancer [26]. Furthermore, CD44 contains an intracellular domain (CD44ICD), which is released in hypoxia by gamma secretase cleavage [27] and binds to HIF-2α [28]. This activates HIF-regulated genes. This study, which was done with glioblastoma cell lines, suggests a positive feedback mechanism in which hypoxia regulates CD44, which in turn may regulate more hypoxia-related genes. We found that cortical astrocytes in the rat brain become CD44+ after an MCA occlusion. In a previous study, CD44 was found to be upregulated in the cortex and striatum of rats after an MCA occlusion, and localized to small blood vessels, macrophages and microglia [29], but the authors did not describe CD44+ in astrocytes.

Seizures

Seizures provoke an increase in CD44 in astrocytes at least in the isocortex and hippocampus, the two areas we examined. Furthermore, transcriptomics of the reactive astrogliosis accompanying temporal lobe epilepsy show upregulated CD44 [15]. The mechanisms underlying this are not known. Hypoxia may be involved, or inflammatory responses. A previous study found CD44 in the mouse hippocampus after pilocarpine-induced seizures, but an astrocyte localization was not described [14].

Regulation of CD44 That Might be Relevant to Studies in the Human CNS

Although the transcriptional regulation of *CD44* has not been studied in human astrocytes, studies with other cultured cell types show that the upstream promoter region of *CD44* is complex, containing binding sites for both positive and negative transcriptional regulators, including sequences that bind AP-1, Nf-kB, Sp1, Egr1, TCF4, ETS-1, p53, KLF4, and Foxp3, the latter three as repressors [30,31]. As noted above, hypoxia regulates *CD44* through HIF-1 α . These studies were carried out in non-CNS cancer cell lines and it is not known whether similar regulations occur in astrocytes, although mouse astrocytes in culture upregulate *CD44* when treated with PMA or TNF α plus gamma interferon [32], and all of these observations suggest that inflammatory conditions may upregulate *CD44*. Which of these transcription factors act to regulate *CD44* in human astrocytes is unknown. In addition, there is evidence for epigenetic regulation of *CD44*. Thus, a 5'-CpG island of *CD44* is methylated in prostate cancer [32]. CpGs are highly methylated in the *CD44*-negative T cell lymphoma line AKR1, although transfection with *c-jun* can activate transcription without major changes in methylation [33]. It will be of interest to examine the methylation status of *CD44* in *CD44*+ and *CD44*-negative astrocytes and investigate if this changes in hypoxia or seizures to allow *CD44* transcription.

There is a Negative Correlation between CD44 and Protoplasmic Astrocyte Genes/Proteins

We previously determined that the *CD44*+ interlaminar astrocytes in the normal human isocortex have lower levels of glutamate transporters and glutamine synthetase than the *CD44*-negative protoplasmic astrocytes [4]. In a mouse model of Alexander disease, a CNS degenerative disorder caused by mutations in *GFAP*, we found that protoplasmic astrocytes of the hippocampus and isocortex became *CD44*+ as the disease progressed [34]. The acquisition of *CD44* correlated strongly with the loss of the glutamate transporter, Glt-1. In a study of the human cingulate gyrus in Huntington disease, RNA sequencing revealed an upregulation of *CD44* during the disease [35]. This study also revealed that astrocytes lost the expression of normal protoplasmic astrocyte genes. Thus, there appears to be a negative correlation between *CD44* and several protoplasmic astrocyte genes and proteins. Whether this correlation is caused by the presence of *CD44* is not known, although testable in future studies. The expression of *CD44* caused by hypoxia and seizures may well alter the physiology of protoplasmic astrocytes in ways that are deleterious to neurons.

Is There Any Value in Downregulating CD44 in Pathological Situations?

If *CD44* plays a role in changing the phenotypes of protoplasmic astrocytes, would there be any value in downregulating *CD44* or preventing its upregulation? Would this preserve a normal protoplasmic astrocyte state? This could be tested in mouse models. In studies of human cancers, *CD44* associates with STAT3, which may lead to STAT3 activation [36]. STAT3 also activates other astrocyte genes, such as *GFAP*, in pathological conditions [37,38]. So et al [36] found that a Vitamin D analog represses *CD44* expression in breast cancer cells. It would be interesting to determine if astrocytes show the same response.

Limitations

Although this is the most thorough study of *CD44*+ astrocytes in the human CNS and we show the conversion of protoplasmic to *CD44*+ astrocytes in hypoxia and epilepsy, our observations do not imply specific molecular mechanisms. Such data on the mechanisms of *CD44* expression appear largely in the cancer biology literature and have not been investigated in astrocytes. The present study is an important background that will promote further investigations by our labs and others.

5. Conclusions

This study includes a number of novel observations, further characterizing the heterogeneity of astrocytes in the human CNS.

1. *CD44*+ astrocytes are present at all levels of the human CNS.
2. Some neurons are surrounded by *CD44*+ processes, including motor neurons, while

isocortical, most diencephalic, and hippocampal neurons are not.

3. CD44+ processes intercalate between ependymal cells at ventricular surfaces.
4. CD44 immunostaining revealed astrocytes in the upper part of the cerebellar molecular layer. These sent processes parallel to the pia and radially toward the Purkinje cell layer.
5. Velate astrocytes of the cerebellar granule cell layer are CD44+.
6. Hypoxia and seizures induce CD44-negative protoplasmic astrocytes to become CD44+.

Supplementary Materials: The following supporting information can be downloaded. Figure S1: Sections through the ependymal lining overlying the subependymal zone in fetal brains to show CD44+ processes between ependymal cells, Figure S2: A coronal section through the lateral and third ventricles shows CD44+ in the anterior commissure (AC), optic tracts (OT), and internal capsule (IC), Figure S3: Sections through the cerebellar cortex, Figure S4: CD44+ positive astrocytes in the Dentate Nucleus (left panels, A,B,C) and Cerebellar Cortex (right panels, D,E,F), Figure S5: In an individual who died with acute hypoxia, isocortical neurons are eosinophilic and shrunken (arrows, A), but astrocytes are not CD44+ (B).

Author Contributions: JEG and OAD conceived of the studies and wrote the paper. YS, YL, OAD, AAS, GM, NA, ESC, CMT, and JEG carried out the studies and edited the manuscript. All authors have read and approved the manuscript.

Funding: The American Brain tumor Association Discover Grant (fully supported by the Uncle Kory Foundation) and the ADRC REC grant (P30AG066462) (OAD), NINDS RO1 NS081333 (CMT).

Institutional Review Board Statement: All investigations were carried out following the rules of the Declaration of Helsinki of 1975. Human brain tissues from patient brain biopsies and autopsies, which were diagnosed based on accepted neuropathological criteria, were obtained from the Department of Pathology and Cell Biology of Columbia University and the New York Brain Bank. All surgeries were performed with the consent of the patients and studies from biopsy tissues are given without any patient identifying information. All autopsy brains were donated after consent from the next of kin or an individual with legal authority to grant such permission. The use of postmortem brain tissues for research was approved by the Columbia University Institutional Review Board with informed consent from patients or their families. The Institutional Review Board has determined that clinicopathologic studies on de-identified postmortem tissue samples are exempt from Human Subject Research according to Exemption 45 CFR 46.104(d)(2).

Informed Consent Statement: Any research article describing a study involving humans should contain this statement. Please add "Informed consent was obtained from all subjects involved in the study." OR "Patient consent was waived due to REASON (please provide a detailed justification)." OR "Not applicable." for studies not involving humans. You might also choose to exclude this statement if the study did not involve humans. Written informed consent for publication must be obtained from participating patients who can be identified (including by the patients themselves). Please state "Written informed consent has been obtained from the patient(s) to publish this paper" if applicable.

Data Availability Statement: We encourage all authors of articles published in MDPI journals to share their research data. In this section, please provide details regarding where data supporting reported results can be found, including links to publicly archived datasets analyzed or generated during the study. Where no new data were created, or where data is unavailable due to privacy or ethical restrictions, a statement is still required. Suggested Data Availability Statements are available in section "MDPI Research Data Policies" at <https://www.mdpi.com/ethics>.

Acknowledgments: The authors greatly appreciate the efforts of members of the Immunostaining Laboratory of the Department of Pathology and Cell Biology at Columbia Irving Medical Center, Dr.

Michael Miller and the staff of the DPCL of the Department of Pathology and Cell Biology for digitizing images, Juncheng Li for technical assistance, and the Neuropathology staff of the Division of Neuropathology for their interest and for many discussions.

Conflicts of Interest: The authors declare no conflict of interest.

References

1. Andriezen, W.L., *The Neuroglia Elements in the Human Brain*. Br Med J, 1893. **2**(1700): p. 227-30.
2. Colombo, J.A., et al., *Immunocytochemical and electron microscope observations on astroglial interlaminar processes in the primate neocortex*. J Neurosci Res, 1997. **48**(4): p. 352-7.
3. Reisin, H.D. and J.A. Colombo, *Astroglial interlaminar processes in human cerebral cortex: variations in cytoskeletal profiles*. Brain Res, 2002. **937**(1-2): p. 51-7.
4. Sosunov, A.A., et al., *Phenotypic heterogeneity and plasticity of isocortical and hippocampal astrocytes in the human brain*. J Neurosci, 2014. **34**(6): p. 2285-98.
5. Falcone, C., et al., *Cortical interlaminar astrocytes across the therian mammal radiation*. J Comp Neurol, 2019. **527**(10): p. 1654-1674.
6. Akiyama, H., et al., *Morphological diversities of CD44 positive astrocytes in the cerebral cortex of normal subjects and patients with Alzheimer's disease*. Brain Res, 1993. **632**(1-2): p. 249-59.
7. Goodison, S., V. Urquidi, and D. Tarin, *CD44 cell adhesion molecules*. Mol Pathol, 1999. **52**(4): p. 189-96.
8. Sosunov, A.A., et al., *Epileptogenic but MRI-normal perituberal tissue in Tuberous Sclerosis Complex contains tuber-specific abnormalities*. Acta Neuropathol Commun, 2015. **3**: p. 17.
9. Girgrah, N., et al., *Localization of the CD44 glycoprotein to fibrous astrocytes in normal white matter and to reactive astrocytes in active lesions in multiple sclerosis*. J Neuropathol Exp Neurol, 1991. **50**(6): p. 779-92.
10. Akpan, N., et al., *Intranasal delivery of caspase-9 inhibitor reduces caspase-6-dependent axon/neuron loss and improves neurological function after stroke*. J Neurosci, 2011. **31**(24): p. 8894-904.
11. Sosunov, A.A., et al., *The mTOR pathway is activated in glial cells in mesial temporal sclerosis*. Epilepsia, 2012. **53 Suppl 1**: p. 78-86.
12. McKhann, G.M., 2nd, et al., *Mouse strain differences in kainic acid sensitivity, seizure behavior, mortality, and hippocampal pathology*. Neuroscience, 2003. **122**(2): p. 551-61.
13. Arai, Y., S. Takashima, and L.E. Becker, *CD44 expression in tuberous sclerosis*. Pathobiology, 2000. **68**(2): p. 87-92.
14. Borges, K., D.L. McDermott, and R. Dingledine, *Reciprocal changes of CD44 and GAP-43 expression in the dentate gyrus inner molecular layer after status epilepticus in mice*. Exp Neurol, 2004. **188**(1): p. 1-10.
15. Pai, B., et al., *High-resolution transcriptomics informs glial pathology in human temporal lobe epilepsy*. Acta Neuropathol Commun, 2022. **10**(1): p. 149.
16. Boer, K., et al., *Gene expression analysis of tuberous sclerosis complex cortical tubers reveals increased expression of adhesion and inflammatory factors*. Brain Pathol, 2010. **20**(4): p. 704-19.
17. Padmashri, R., et al., *Modeling human-specific interlaminar astrocytes in the mouse cerebral cortex*. J Comp Neurol, 2021. **529**(4): p. 802-810.
18. Nowakowski, T.J., et al., *Transformation of the Radial Glia Scaffold Demarcates Two Stages of Human Cerebral Cortex Development*. Neuron, 2016. **91**(6): p. 1219-1227.
19. Miletti-González, K.E., et al., *Identification of function for CD44 intracytoplasmic domain (CD44-ICD): modulation of matrix metalloproteinase 9 (MMP-9) transcription via novel promoter response element*. J Biol Chem, 2012. **287**(23): p. 18995-9007.
20. Mirzadeh, Z., et al., *Neural stem cells confer unique pinwheel architecture to the ventricular surface in neurogenic regions of the adult brain*. Cell Stem Cell, 2008. **3**(3): p. 265-78.
21. Sanai, N., et al., *Unique astrocyte ribbon in adult human brain contains neural stem cells but lacks chain migration*. Nature, 2004. **427**(6976): p. 740-4.
22. Quiñones-Hinojosa, A., et al., *Cellular composition and cytoarchitecture of the adult human subventricular zone: a niche of neural stem cells*. J Comp Neurol, 2006. **494**(3): p. 415-34.
23. Chan-Palay, V. and S.L. Palay, *The form of velate astrocytes in the cerebellar cortex of monkey and rat: high voltage electron microscopy of rapid Golgi preparations*. Z Anat Entwicklungsgesch, 1972. **138**(1): p. 1-19.
24. Ramon y Cajal, S., *Histology of the Nervous System*. Vol. 2. 1995, New York: Oxford University Press.
25. Krishnamachary, B., et al., *Hypoxia regulates CD44 and its variant isoforms through HIF-1α in triple negative breast cancer*. PLoS One, 2012. **7**(8): p. e44078.
26. Liang, G., et al., *Hypoxia regulates CD44 expression via hypoxia-inducible factor-1α in human gastric cancer cells*. Oncol Lett, 2017. **13**(2): p. 967-972.

27. Pietras, A., et al., *Osteopontin-CD44 signaling in the glioma perivascular niche enhances cancer stem cell phenotypes and promotes aggressive tumor growth*. *Cell Stem Cell*, 2014. **14**(3): p.357-69.
28. Johansson, E., et al., *CD44 Interacts with HIF-2 α to Modulate the Hypoxic Phenotype of Perinecrotic and Perivascular Glioma Cells*. *Cell Rep*, 2017. **20**(7): p. 1641-1653.
29. Wang, H., et al., *Use of suppression subtractive hybridization for differential gene expression in stroke: discovery of CD44 gene expression and localization in permanent focal stroke in rats*. *Stroke*, 2001. **32**(4): p.1020-7.
30. Zhang, C., et al., *FOXP3 suppresses breast cancer metastasis through downregulation of CD44*. *Int J Cancer*, 2015. **137**(6): p. 1279-90.
31. Chen, C., et al., *The biology and role of CD44 in cancer progression: therapeutic implications*. *J Hematol Oncol*, 2018. **11**(1): p. 64.
32. Haegel, H., et al., *Activated mouse astrocytes and T cells express similar CD44 variants. Role of CD44 in astrocyte/T cell binding*. *J Cell Biol*, 1993. **122**(5): p. 1067-77.
33. Hyman, R., *Lack of a consistent relationship between demethylation of the CD44 promoter and CD44 expression*. *Immunogenetics*, 2002. **53**(10-11): p. 914-24.
34. Sosunov, A.A., et al., *Phenotypic conversions of "protoplasmic" to "reactive" astrocytes in Alexander disease*. *J Neurosci*, 2013. **33**(17): p. 7439-50.
35. Al-Dalahmah, O., et al., *Single-nucleus RNA-seq identifies Huntington disease astrocyte states*. *Acta Neuropathol Commun*, 2020. **8**(1): p. 19.
36. So, J.Y., et al., *Targeting CD44-STAT3 signaling by Gemini vitamin D analog leads to inhibition of invasion in basal-like breast cancer*. *PLoS One*, 2013. **8**(1): p. e54020.
37. Xu, Z., et al., *Role of signal transducer and activator of transcription-3 in up-regulation of GFAP after epilepsy*. *Neurochem Res*, 2011. **36**(12): p. 2208-15.
38. O'Callaghan, J.P., et al., *Early activation of STAT3 regulates reactive astrogliosis induced by diverse forms of neurotoxicity*. *PLoS One*, 2014. **9**(7): p. e102003.

Disclaimer/Publisher's Note: The statements, opinions and data contained in all publications are solely those of the individual author(s) and contributor(s) and not of MDPI and/or the editor(s). MDPI and/or the editor(s) disclaim responsibility for any injury to people or property resulting from any ideas, methods, instructions or products referred to in the content.